UNCLASSIFIED
DOES NOT CONTAIN
UNCLASSIFIED CONTROLLED
NUCLEAR INFORMATION

ADC &
Reviewing
Official: MK Harris
(Mary K. Harris, Manager)

Date: 10/24/02

Key Words:
Engineered Trench
B-25 Containers
Dynamic Compaction
Low-Level Waste Disposal

Retention:
Permanent

FINITE ELEMENT ANALYSIS ENHANCEMENT FOR B-25 CONTAINER DYNAMIC COMPACTION (U)

C. Gong and W. E. Jones

SEPTEMBER 2002

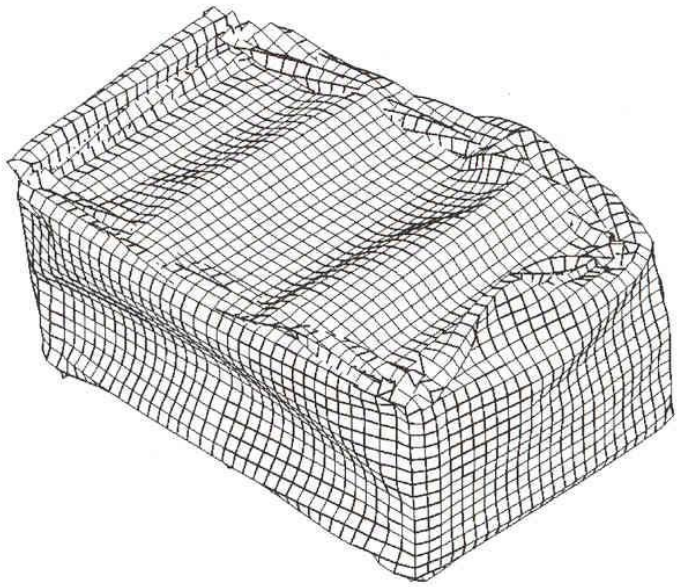

Westinghouse Savannah River Company
Savannah River Site
Aiken, SC 29808

Prepared for the U.S. Department of Energy Under Contract Number DE-AC09-96SR18500

SRS savannah river site ™

This document was prepared in conjunction with work accomplished under Contract No. DE-AC09-96SR18500 with the U. S. Department of Energy.

DISCLAIMER

This report was prepared as an account of work sponsored by an agency of the United States Government. Neither the United States Government nor any agency thereof, nor any of their employees, makes any warranty, express or implied, or assumes any legal liability or responsibility for the accuracy, completeness, or usefulness of any information, apparatus, product or process disclosed, or represents that its use would not infringe privately owned rights. Reference herein to any specific commercial product, process or service by trade name, trademark, manufacturer, or otherwise does not necessarily constitute or imply its endorsement, recommendation, or favoring by the United States Government or any agency thereof. The views and opinions of authors expressed herein do not necessarily state or reflect those of the United States Government or any agency thereof.

This report has been reproduced directly from the best available copy.

Available for sale to the public, in paper, from: U.S. Department of Commerce, National Technical Information Service, 5285 Port Royal Road, Springfield, VA 22161,
phone: (800) 553-6847,
fax: (703) 605-6900
email: orders@ntis.fedworld.gov
online ordering: http://www.ntis.gov/help/index.asp

Available electronically at http://www.osti.gov/bridge
Available for a processing fee to U.S. Department of Energy and its contractors, in paper, from: U.S. Department of Energy, Office of Scientific and Technical Information, P.O. Box 62, Oak Ridge, TN 37831-0062,
phone: (865)576-8401,
fax: (865)576-5728
email: reports@adonis.osti.gov

WSRC-TR-2002-00353

Key Words:
Engineered Trench
B-25 Containers
Dynamic Compaction
Low-Level Waste Disposal

Retention:
Permanent

FINITE ELEMENT ANALYSIS ENHANCEMENT FOR B-25 CONTAINER DYNAMIC COMPACTION (U)

Chung Gong and William E. Jones
Savannah River Technology Center

SEPTEMBER 2002

Westinghouse Savannah River Company
Savannah River Site
Aiken, SC 29808

Prepared for the U.S. Department of Energy Under
Contract Number DE-AC09-96SR18500

REVIEWS AND APPROVALS

William E. Jones for Chung Gong 10/24/02

Chung Gong, Author — Date
Engineering Modeling & Simulation Group,
Engineering Development Section (Retired)

William E. Jones 10/24/02

William E. Jones, Author — Date
Geo-Modeling Group,
Environmental Restoration Technology Section

Tsu-Te Wu 10/25/02

Tsu-Te (Alan) Wu, Technical Reviewer — Date
Engineering Modeling & Simulation Group,
Engineering Development Section

Cynthia P. Holding-Smith 10/30/02

Cynthia P. Holding-Smith, Manager — Date
Engineering Modeling & Simulation Group,
Engineering Development Section

M K Harris 11/4/02

Mary K. Harris, Manager — Date
Geo-Modeling Group,
Environmental Restoration Technology Section

Robert C Aylward 10/30/02

Robert C. Aylward, Manager — Date
Environmental Restoration Technology Section

TABLE OF CONTENTS

LIST OF FIGURES ..... **iii**
1.0 INTRODUCTION **1**
2.0 MODELING DYNAMIC COMPACTION **3**
2.1 ADDING SOIL TO THE UPPERMOST B-25 ..... **9**
2.2 ADDITIONAL MODELS WITH UPPERMOST B-25 HALF-FULL OF SOIL **25**
2.3 INCORPORATING STEEL-VOLUME LOSS (CORROSION) **39**
3.0 CONCLUSIONS **45**
4.0 REFERENCES **47**

LIST OF FIGURES

Figure 1. Initial dynamic compaction model with overlying soil layer. Non-reflective boundary conditions were later added to the overlying and underlying soil layers. 4
Figure 2. Extreme element deformation in overlying soil layer. (Neither underlying nor overlying soils have non-reflective boundaries.) 5
Figure 3. Close-up view of undeformed 4-ft-thick soil layer 6
Figure 4. Close-up view of deformed overlying soil layer after first impact event 7
Figure 5. Color-enhanced depiction of overlying soil layer deformation 8
Figure 6. Uppermost B-25 half-full of soil, with wave-reflective soil foundation 10
Figure 7. Four B-25 containers on soil foundation with non-reflective boundary (no soil within uppermost B-25) 11
Figure 8. B-25 containers on soil with non-reflective boundary after dynamic compaction event (no soil within uppermost B-25) 12
Figure 9. B-25s after dynamic compaction event (soil foundation not shown) 13
Figure 10. Top view of the deformed lowermost B-25 (Box 1) 14
Figure 11. Bottom view of the lowermost B-25 (Box 1) 15
Figure 12. Top view of the deformed middle bottom B-25 (Box 2) 16
Figure 13. Bottom view of the middle bottom B-25 (Box 2) 17
Figure 14. Top view of top middle B-25 (Box 3) 18
Figure 15. Bottom view of the top middle B-25 (Box 3) 19
Figure 16. Top view of the deformed uppermost B-25 (Box 4) 20
Figure 17. Bottom view of the deformed uppermost B-25 21
Figure 19. Strain -energy time history for whole model 23
Figure 18. Strain-energy time history for stack of four B-25s and containerized waste 24
Figure 20. Refined dynamic compaction model with non-reflective boundary elements surrounding the 4-ft-thick soil layer and beneath the underlying soil 26
Figure 21. The 4-ft-thick soil layer with surrounding non-reflective elements 27
Figure 22. Deformation of the 4-ft-thick soil layer with undeformed lateral elements 28
Figure 23. Deformed 4-ft-thick soil layer (non-reflective lateral elements not shown) 29

Figure 24. Non-reflective lateral elements prior to dynamic compaction event 30
Figure 25. Affected non-reflective lateral elements subsequent to the dynamic compaction event 31
Figure 26. Colorized version of soil layer deformation 32
Figure 27. Four B-25s modeled with uppermost B-25 half-full of soil, half-full of waste, with soil foundation underlain by non-reflective barrier 33
Figure 28. Deformed B-25s after dynamic compaction event. Uppermost B-25 appears to bulge upward due to presence of waste and soil within this B-25. 34
Figure 29. Top view of uppermost B-25. Top of B-25 appears to bulge upward due to presence of waste and soil within this B-25. 35
Figure 30. Bottom view of deformed uppermost B-25 36
Figure 31. Undeformed uppermost B-25 prior to dynamic compaction event, and deformed uppermost B-25 after dynamic compaction event (includes waste in the bottom half and soil in the top half) 37
Figure 32. Color depiction of first principal strain in uppermost B-25 after dynamic compaction event (includes waste in the bottom half and soil in the top half) 38
Figure 33. Dynamic compaction results after steel-volume reduction in lower two B-25s 40
Figure 34. Top view of the lowermost B-25 (Box 1) 41
Figure 35. Bottom view of the lowermost B-25 (Box 1) 42
Figure 36. Bottom view of the second-from-bottom B-25 (Box 2) 43
Figure 37. Top view of the second-from-bottom B-25 (Box 2) 44

1.0 INTRODUCTION

Gong (2001) describes initial structural finite element modeling for dynamic compaction of B-25 containers buried in Engineered Trench #1 at the U.S. Department of Energy's Savannah River Site (SRS), Aiken, South Carolina. Dynamic compaction is the practice of dropping a heavy weight to compact material that has been placed in the subsurface for disposal. B-25s placed in Engineered Trench #1 contain low-level radioactive waste. B-25 containers are 4 ft. x 4 ft. x 6 ft., low-carbon, 12- to 14-gauge steel containers with a non-hinged lid. [See Jones and Li (2002) for additional information.] Dynamic compaction of buried B-25s is an option that could mitigate subsidence of the cap that is eventually constructed over an engineered trench disposal site.

The objective of numerical modeling of the Engineered trench system was to evaluate the response of B-25 containers to dynamic compaction, eventually incorporating dynamic compaction behavior with various degrees of B-25 corrosion. Understanding the structural behavior of buried B-25s over time is important for anticipating and dealing with subsidence. Subsidence may compromise the long-term integrity of the caps placed over the buried waste to limit downward water and contaminant movement through the material.

The initial numerical modeling of the B-25 containers' dynamic compaction (Gong 2001) provides a wide range of parametric investigations, describes the limitations of geometric and material modeling capability, and, in particular, establishes the bridge between physical reality and mathematical modeling. The present report documents additional considerations to the initial structural finite element modeling efforts related to dynamic compaction. A few essential considerations were developed immediately prior to the first author's retirement from SRS in May 2002. Meetings with the SRS Solid Waste Division in April 2002 indicated that the modeling should include static or quasi-static modeling of B-25 structural behavior, since dynamic compaction may not be performed. Those modeling efforts are currently being performed by Dr. Alan Wu, with the Savannah River Technology Center, and will be presented in a separate report (Wu, 2002).

Per the B-25 Procurement Specification C-SPP-G-00101, Rev. 5, dated May, 2001, the current modeling effort assumes the B-25s placed in the Engineered Trench #1 (ET) are 12-gauge (0.1094 inch thickness) steel construction. The B-25 exhumed for the study was apparently procured under a previous specification calling for 14-gauge steel. Recent ET Phase 1 photos from SRS Solid Waste Division (SWD) indicate containers that are actually being disposed include B-12s, B-25s of varying construction, steel containers several times the size of B-25s, and 55-gallon drums. Given the variation in waste containers, structural finite element modeling is limited to modeling B-25 behavior for a "typical" stack or several adjacent stacks of B-25 containers. For engineering problems with numerous uncertainties in the physical and geometrical parameters, the exact solutions can never be obtained. Nevertheless, with thorough understanding of the numerical tool and the physics and mechanics of the engineering system, the bounding (upper-bound and lower-bound) solutions can be developed.

This page intentionally left blank.

2.0 MODELING DYNAMIC COMPACTION

Initial dynamic compaction finite-element modeling efforts are described in Gong (2001). Additional considerations to the Fiscal Year (FY) 2001 dynamic compaction modeling in FY 2002, immediately prior to the first author's retirement from Savannah River Site, are included in this report. The first case considered comprises adding the 4-ft-thick interim soil cover layer to investigate its effect on dynamic compaction. The top layer of soil is not confined. In the realistic physical situation, the topsoil layer is surrounded by the neighboring soil media that provide partial confinement to the soil layer in the center. However, the true physical confinement exerted upon the soil mass in the problem cannot be determined without full-scale modeling of the whole engineering system.

The strength of a soil structure is characteristically derived from the confinement (in other words, the hydrostatic pressure in the soil element) developed in the soil mass. Without sufficient hydrostatic pressure in the soil element, the soil structure has little (from cohesive strength) or no strength at all. The results appeared realistic, in that the soil was compacted and the underlying containers were relatively unaffected. Since the soil elements on the top of the soil layer are extremely weak, the elements are flattened under the dynamic impact. After the finite elements drastically deformed the volume of a distorted approaches zero that will incur numerical instability in the calculation. Consequently the calculation stops as any of the elements is excessively distorted. Figure 1 through Figure 5 exhibit the finite element models and the deformation configurations.

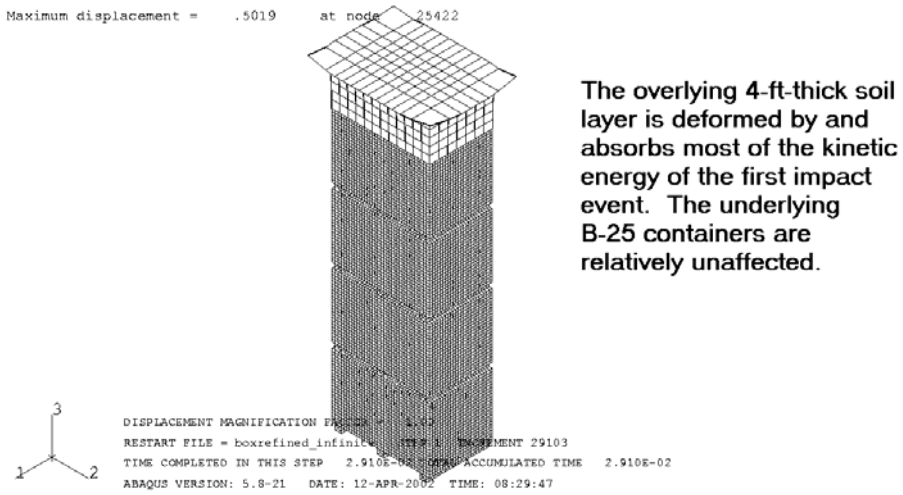

Figure 1. Initial dynamic compaction model with overlying soil layer. Non-reflective boundary conditions were later added to the overlying and underlying soil layers.

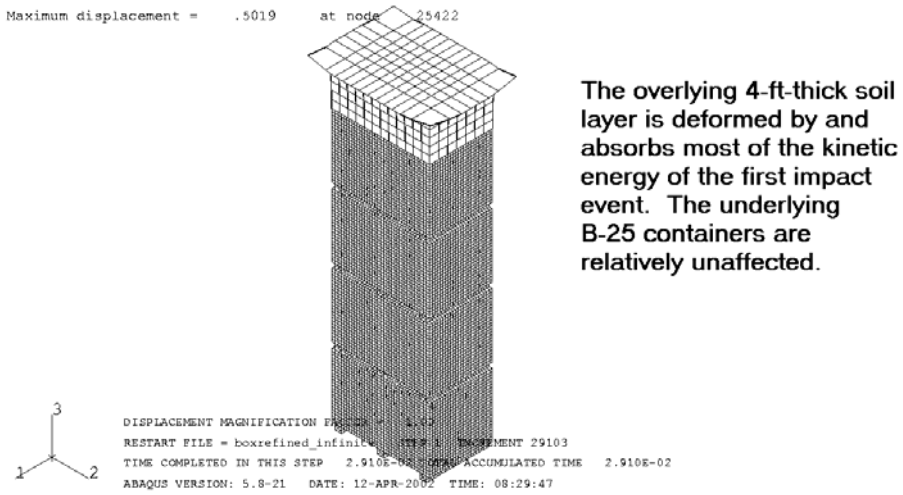

Figure 2. Extreme element deformation in overlying soil layer. (Neither underlying nor overlying soils have non-reflective boundaries.)

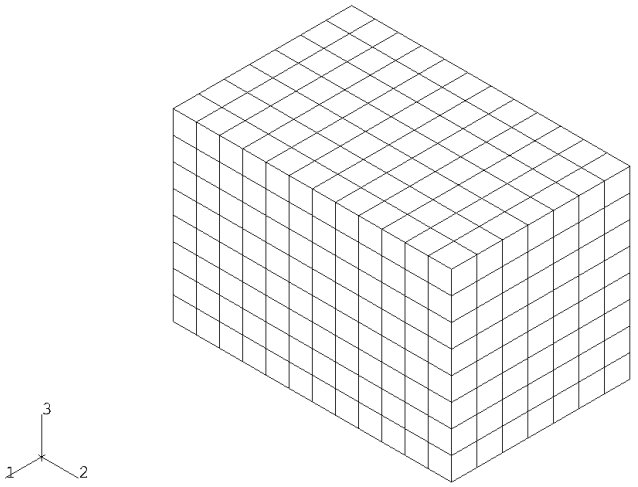

Close-up view of
undeformed
4-ft-thick soil layer.

Figure 3. Close-up view of undeformed 4-ft-thick soil layer

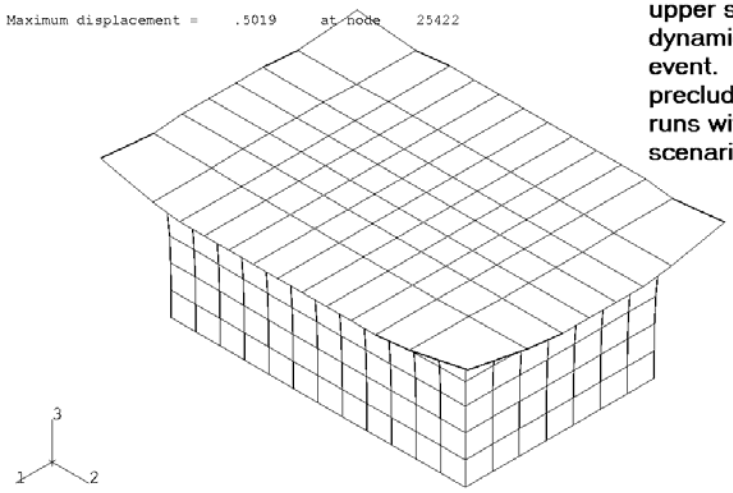

Close-up view of deformed upper soil layer after single dynamic compaction impact event. Element deformation precluded additional model runs without modifying this scenario.

Figure 4. Close-up view of deformed overlying soil layer after first impact event

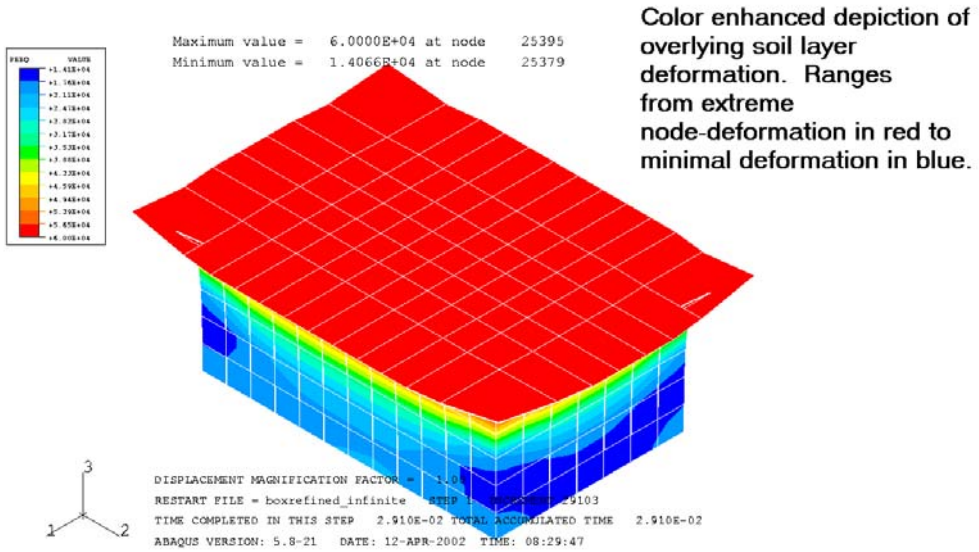

Figure 5. Color-enhanced depiction of overlying soil layer deformation

2.1 ADDING SOIL TO THE UPPERMOST B-25

A B-25 exhumed from beneath eight feet of soil in 2001 had its lid pushed within the B-25 and covered with soil (Jones and Li, 2001). All void space in the buried B-25 was filled with water. Yau (1986) indicates a B-25 lid (14-gauge construction) could begin to deflect under 0.3 ft of soil, and collapse under 10.5 ft of soil. Dames and Moore (1987) indicates buckling of a 14-gauge B-25 lid would occur with as little as 3.3 ft of overlying soil. These physical and theoretical observations point to the necessity for knowing how soil behaves in a confined container under dynamic compaction. A model of the B-25 stack with soil within the top half and waste within the bottom half of the uppermost B-25 is presented.

As discussed in Gong (2001), mathematical modeling of real materials has its limits. In a real unsaturated medium, the soil possesses a measurable amount of compressibility. The soil structure under dynamic impact is mostly in the plastic state. Mathematical modeling of soil in the plastic state utilizes the incompressibility characteristics of the soil (such as the soil is in the saturated condition).

For the modeling presented here, the lid is considered attached to the B-25 wall along the four edges. If the lid in this model were detached from the container wall, the soil inside the B-25 would squeeze out. In the excavated B-25, the top lid was opened (pushed within the container); i.e., in reality, the lid is detached from the container walls. The quasi-static finite element analysis described in Wu (2002) uses the ‘detached lid’ approach. Modeling the waste is different from modeling the soil, and the mechanical behavior of the waste is accordingly different from the soil. Detailed discussion can be found in (Gong, 2001).

The incompressibility of soil in the initial attempt of the model with the uppermost B-25 half-full of waste and half-full of soil produced results that appeared contrary to common sense. Also the lowermost B-25 appeared overly compressed. In the dynamic compaction process, the impact impulse from the impact weight generates a compressive mechanical wave in the B-25s. Comparatively, the mechanical waves travel faster in the metal than in the non-metal materials. Therefore, the waves propagate mostly along the metal walls of the boxes to the bottom of the soil foundation. In the finite element model, the bottom of the soil foundation is fixed and the shallow soil foundation will not absorb much dynamic energy. Consequently, a great deal of kinetic energy is reflected back to the boxes. The strong reflected compressive waves associated with the downward impact impulse render a heavy blow to the bottom box. The results for this dynamic compaction modeling approach are shown in Figure 6.

To remedy this apparent anomaly, the model was enhanced with a larger, non-reflective soil base. The non-reflective soil base would not allow compression waves to reflect back into stack of B-25 containers. The modification was run without soil in the uppermost B-25. (Figure 7 through Figure 17)

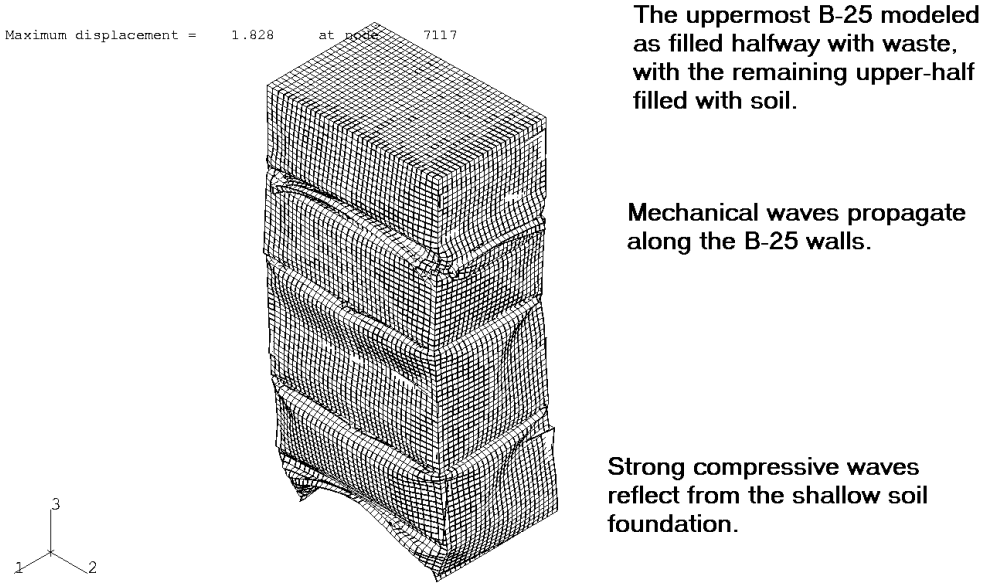

Figure 6. Uppermost B-25 half-full of soil, with wave-reflective soil foundation

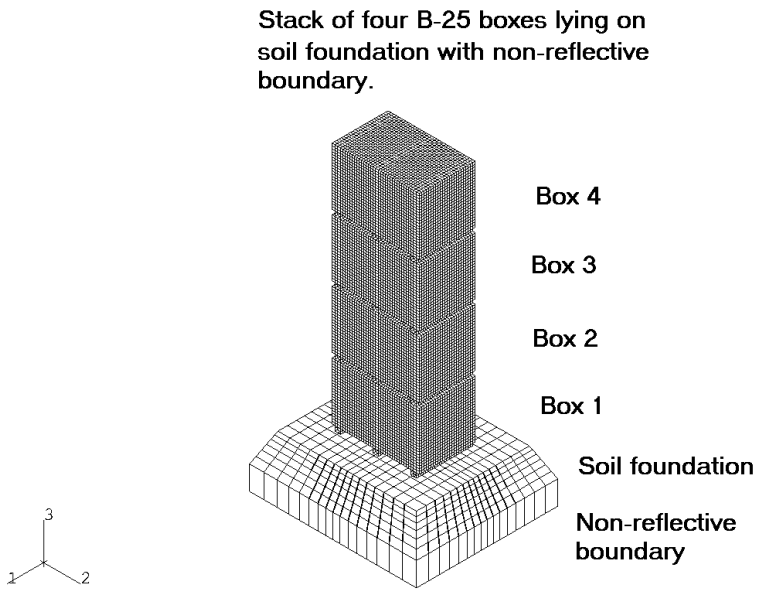

Figure 7. Four B-25 containers on soil foundation with non-reflective boundary (no soil within uppermost B-25)

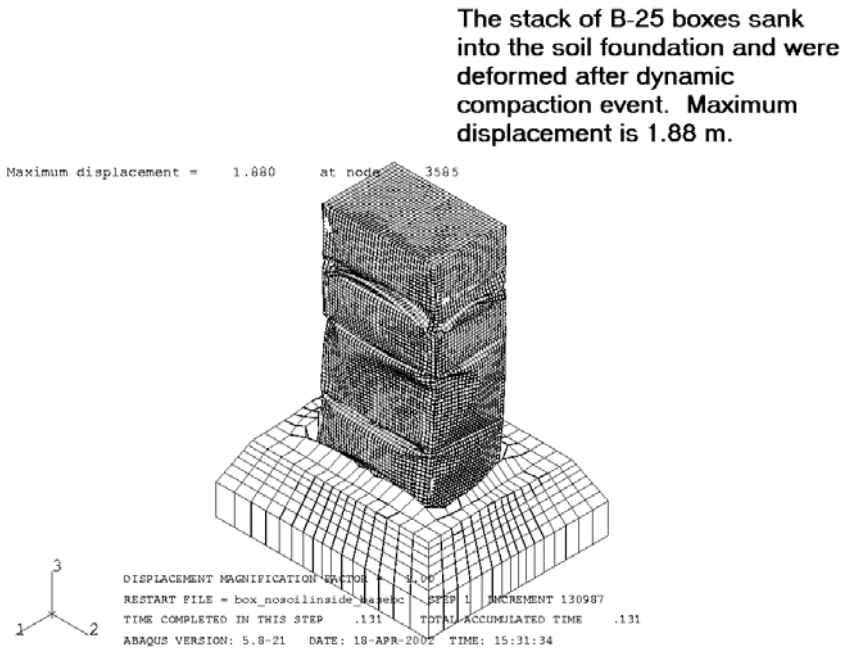

Figure 8. B-25 containers on soil with non-reflective boundary after dynamic compaction event (no soil within uppermost B-25)

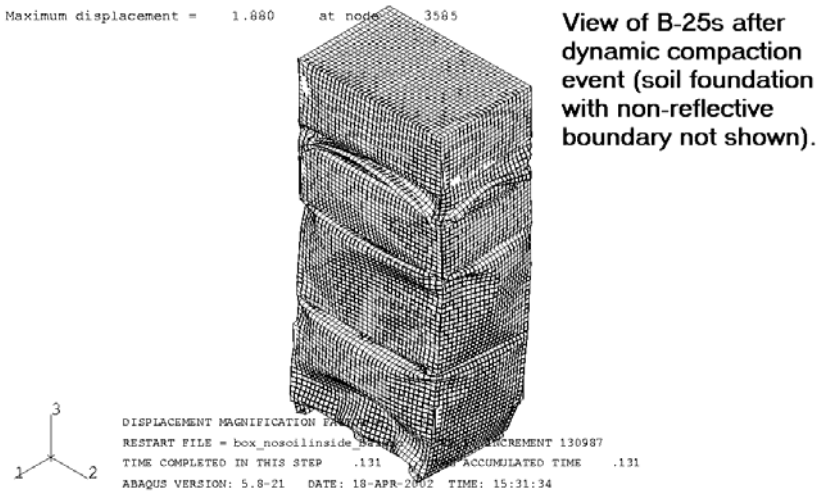

Figure 9. B-25s after dynamic compaction event (soil foundation not shown)

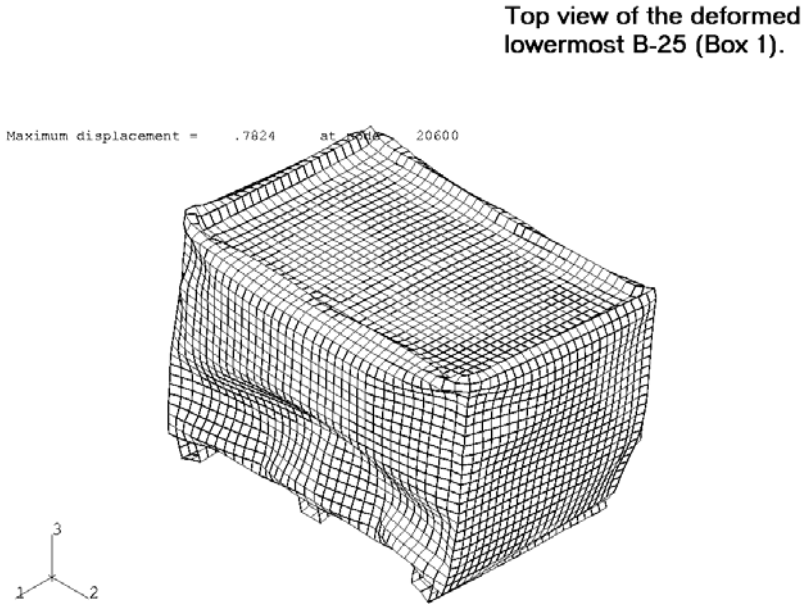

Figure 10. Top view of the deformed lowermost B-25 (Box 1)

Bottom view of the deformed lowermost B-25 (Box 1).

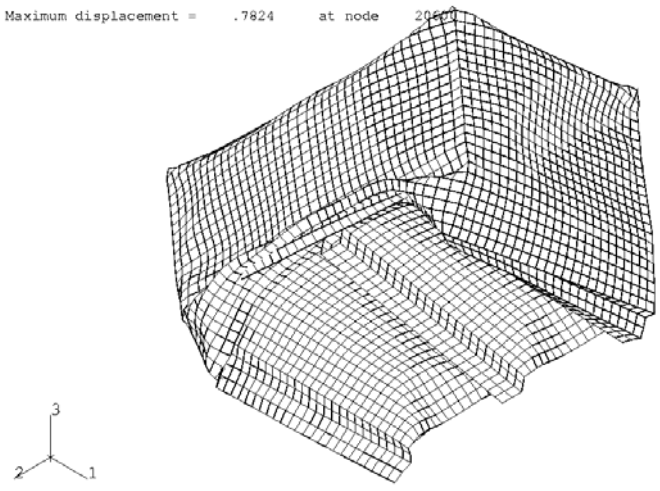

Figure 11. Bottom view of the lowermost B-25 (Box 1)

Top view of the deformed
middle bottom B-25 (Box 2).

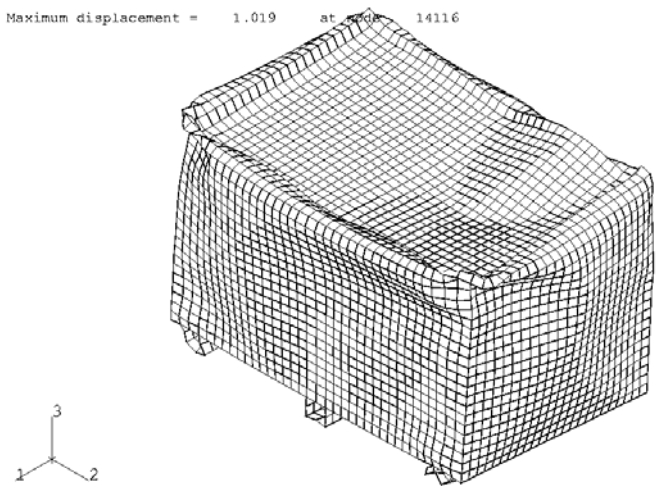

Figure 12. Top view of the deformed middle bottom B-25 (Box 2)

Bottom view of the deformed middle bottom B-25 (Box 2).

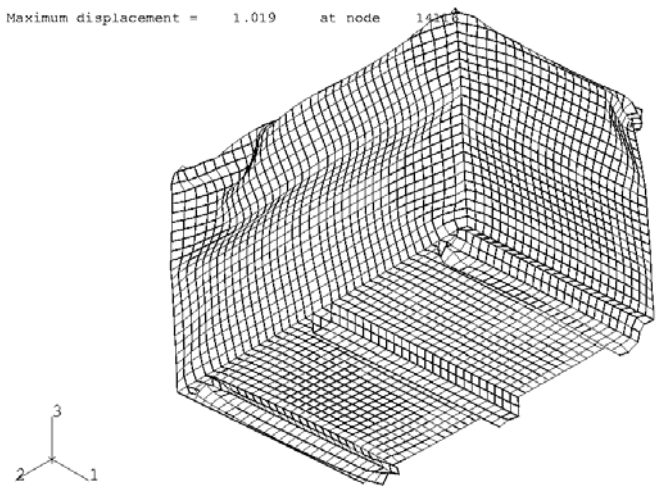

Figure 13. Bottom view of the middle bottom B-25 (Box 2)

Top view of the deformed top middle B-25 (Box 3).

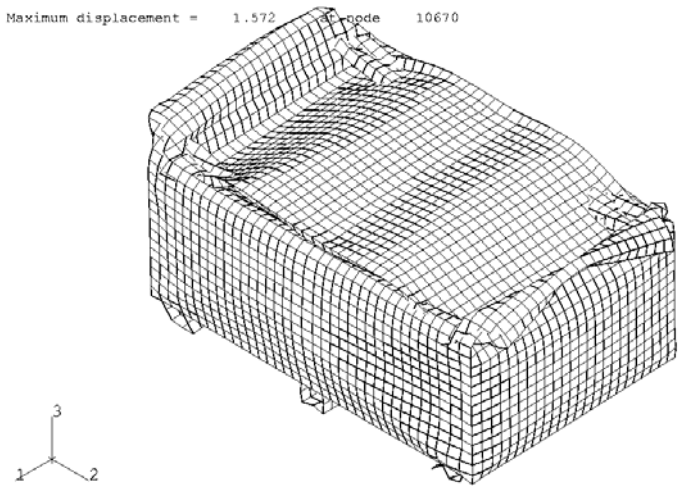

Figure 14. Top view of top middle B-25 (Box 3)

Bottom view of the deformed top middle B-25 (Box 3).

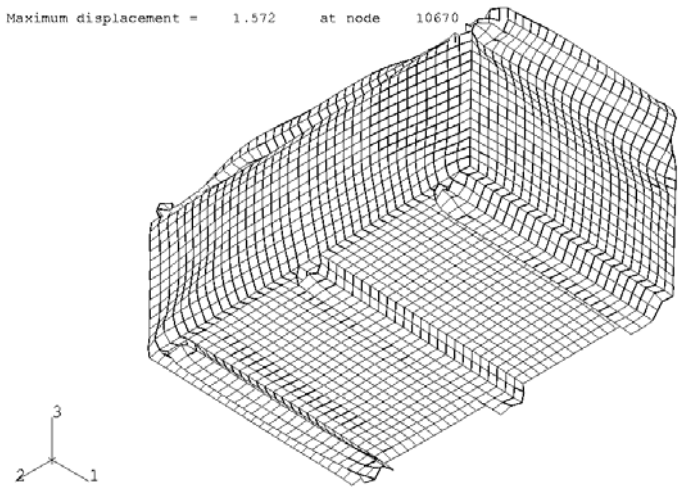

Figure 15. Bottom view of the top middle B-25 (Box 3)

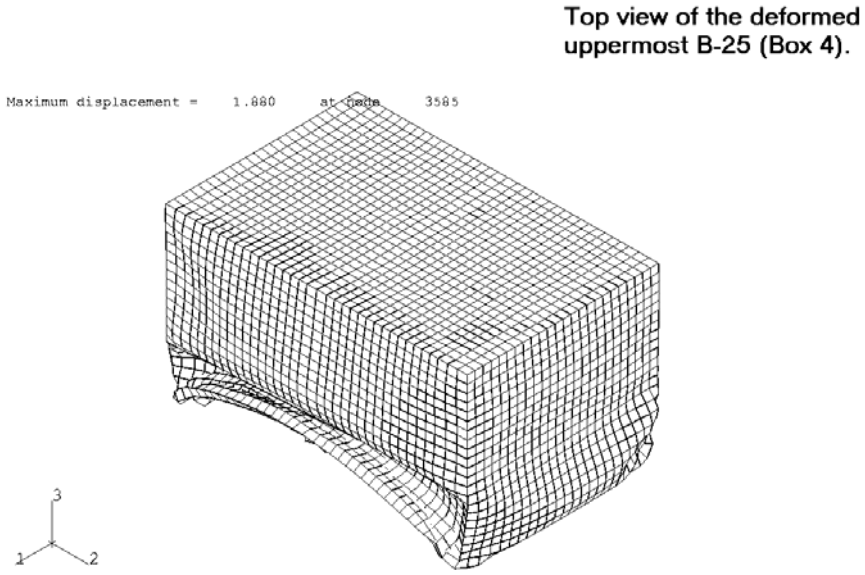

Figure 16. Top view of the deformed uppermost B-25 (Box 4)

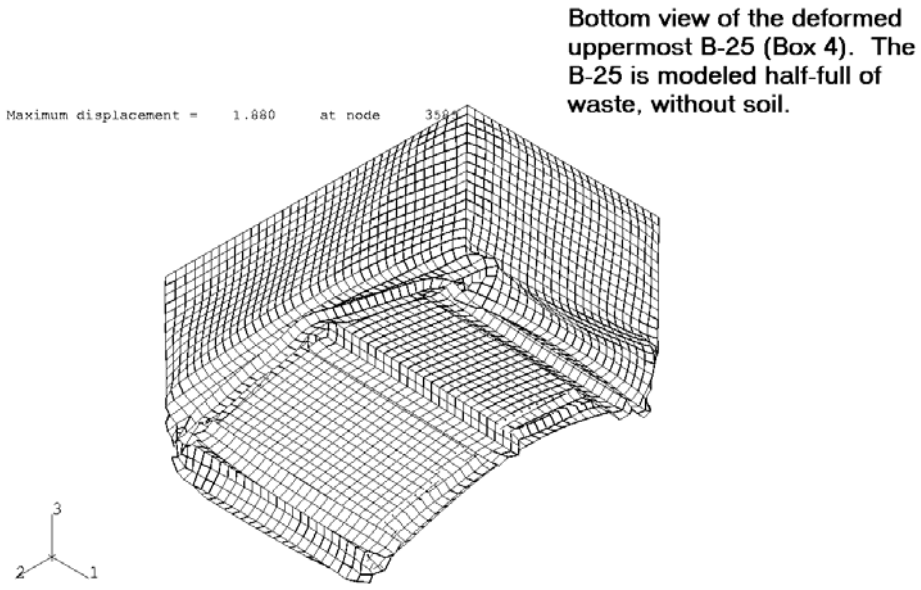

Figure 17. Bottom view of the deformed uppermost B-25

The non-reflective boundary element used is derived for linear analysis. The material mechanical properties during the compaction process should be maintained constant. In this analysis, the soil mechanical properties vary with the magnitude of the nuclear compression in the soil elements. The non-reflective boundary elements adopted by the initial mechanical properties of the soil are not effective in removing the reflection from the bottom of the soil foundation. Since the initial soil mechanical strength is relatively weak, when heavy compressive waves reach the soil foundation, the soil is solidified and stiffens. The weak non-reflective boundary element is incapable of removing the reflected waves. A variable, non-reflective boundary element can be derived and implemented into the finite element program in the future.

Strain-energy time histories for the dynamic compaction impact event for the model illustrated in Figure 7 through Figure 17 are presented in Figure 19 and Figure 18. Figure 18 shows the energy history for the whole system, including the impact weight, B-25s, waste, and non-reflective soil foundation. Figure 19 shows the energy history for the B-25s and containerized waste.

The time history plots of the energies in this dynamic system are similar to those reported in (Gong 2001, Figures 26, 27). The discussion in the previous report is also valid for the time history of energies depicted in this report. Nonetheless, the slight effect of the non-reflective boundary elements delay the responses of the B-25 container system. As expounded in the previously, the non-reflective boundary elements are ineffective due to the fact that the elasticity parameters in the non-reflective elements cannot match up with the soil foundation stiffness during the dynamic compaction process. If it is desired that the strong reflection of the compressive wave must be removed, the elasticity parameters in the non-reflective elements can be beefed-up to the strength of the soil foundation at the moment of strong reflection. This is a part of the iterative nature of parametric analysis in improving problem-solving results. The capabilities of the numerical modeling tools are limited, however, the intelligence and imagination for utilizing these tools are unlimited.

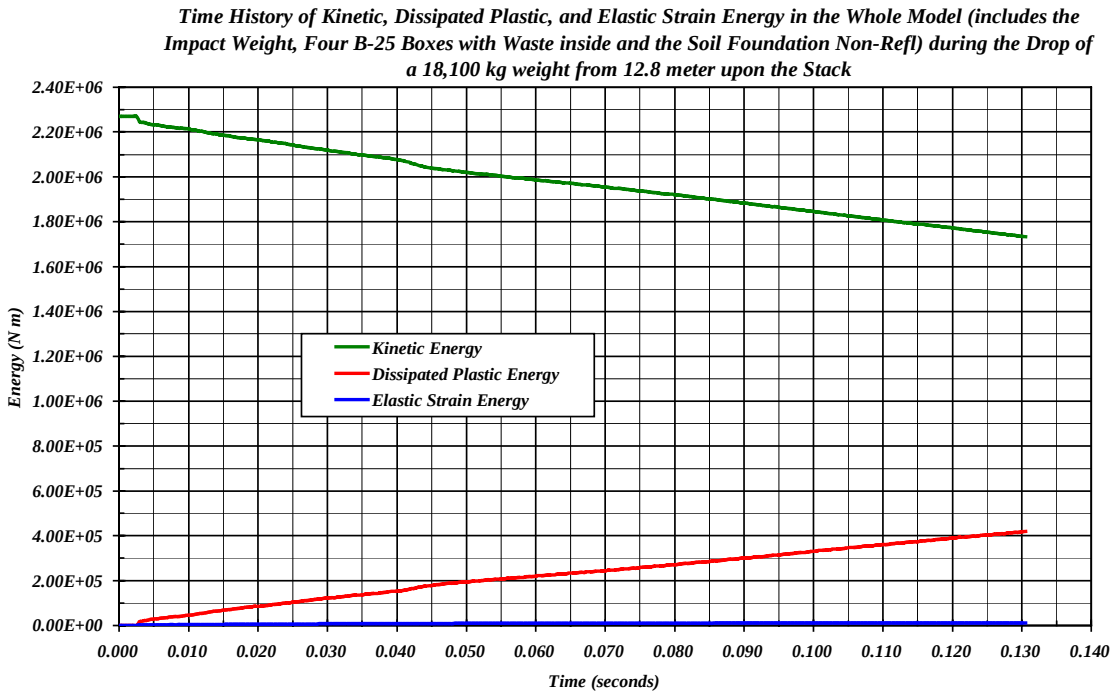

Figure 18. Strain -energy time history for whole model

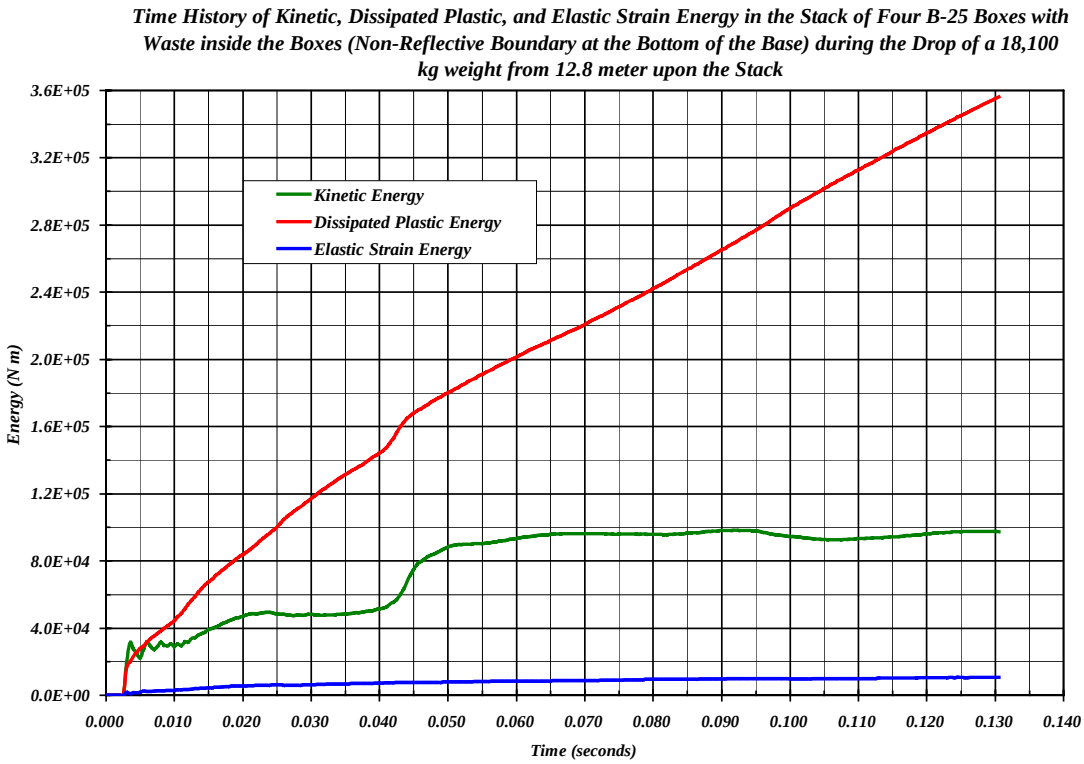

Figure 19. Strain-energy time history for stack of four B-25s and containerized waste

2.2 ADDITIONAL MODEL S WITH UPPERMOST B-25 HALF-FULL OF SOIL

Two additional models were run with the uppermost B-25 half-full of waste and half-full of soil. One version shows reduced compression of the overlying soil layer with little compression of the B-25s (Figure 20 through Figure 26). This version includes non-reflective boundaries for both the soil foundation and the overlying soil layer. The other version shows an interesting upward deformation of the uppermost B-25 lid due to compression of the contained materials (Figure 27 through Figure 32). The latter model is run without an overlying soil layer to show the effect of dynamic compression on the B-25s rather than just compression of the overlying soil layer.

The overlying soil layer on the top of the uppermost B-25 box is surrounded by the adjacent soil mass. Mechanically, the surrounding soil mass will absorb and dissipate most of the energy impinging from the overlying soil layer when the layer is under dynamic impact. Therefore, modeling the surrounding boundary of the overlying soil layer with a non-reflective boundary element is necessary. Unfortunately, besides the elasticity parameter shortcoming mentioned previously, the non-reflective boundary elements are ineffective for non-normal incident waves. (Detailed discussion of various non-reflective boundary elements is beyond the scope of this report.)

The non-reflective boundary elements certainly provide measurable confinement for the overlying soil layer. The deformation of the layer is decreased significantly. Again, due to extreme soil element distortion in the top layer the computation cannot continue.

The soil confinement inside the uppermost B-25 box has been discussed in previous sections. In Figure 28 to Figure 32, the top B-25 box is drastically deformed, while volume of the box changes only slightly (by visual inspection). The waste and soil models in this calculation are both relatively incompressible in the plastic stress state. If it is necessary, the material models in the computer program can be modified (with user-supplied material models).

All these parametric studies extend and enhance the understanding of the problem and the modeling tools. Within the limitations an optimized solution can be derived.

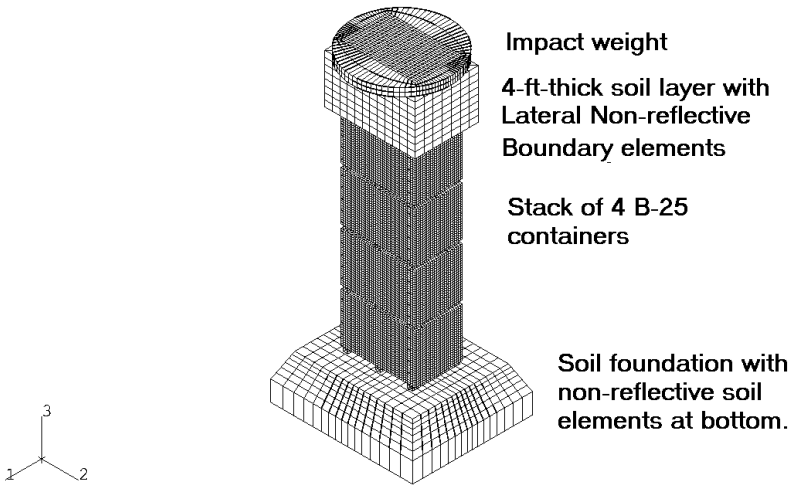

Figure 20. Refined dynamic compaction model with non-reflective boundary elements surrounding the 4-ft-thick soil layer and beneath the underlying soil

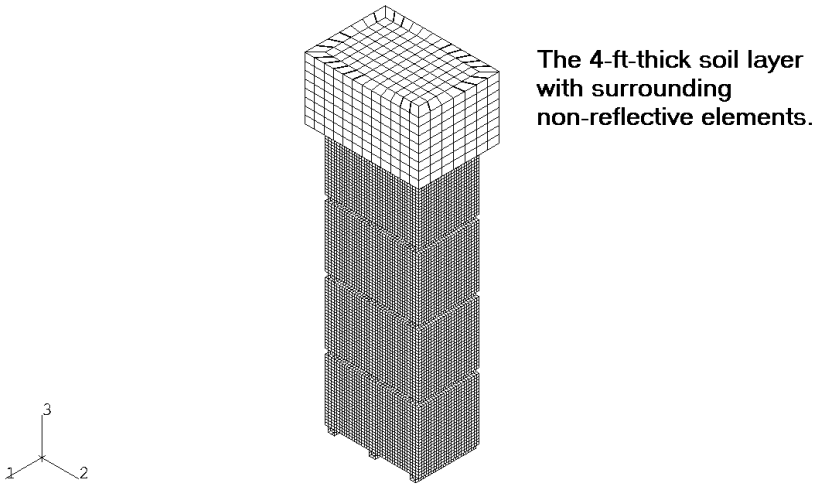

Figure 21. The 4-ft-thick soil layer with surrounding non-reflective elements

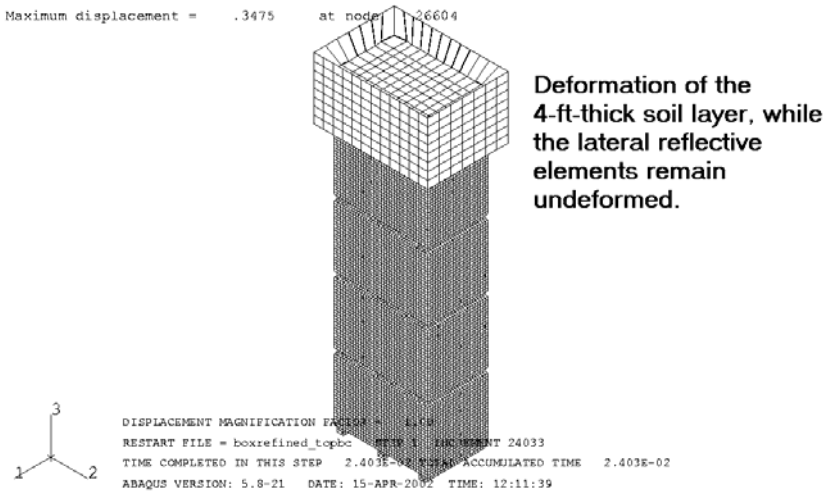

Figure 22. Deformation of the 4-ft-thick soil layer with undeformed lateral elements

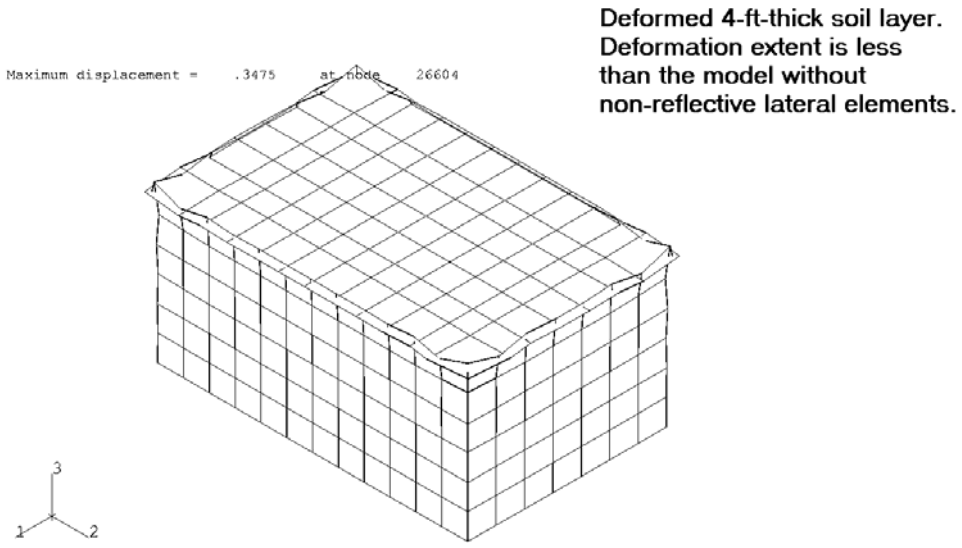

Figure 23. Deformed 4-ft-thick soil layer (non-reflective lateral elements not shown)

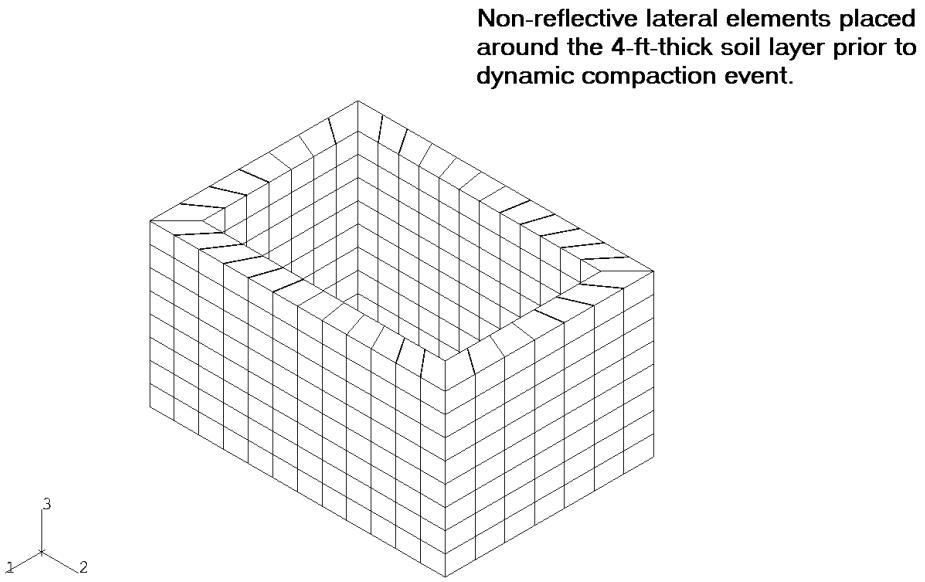

Figure 24. Non-reflective lateral elements prior to dynamic compaction event

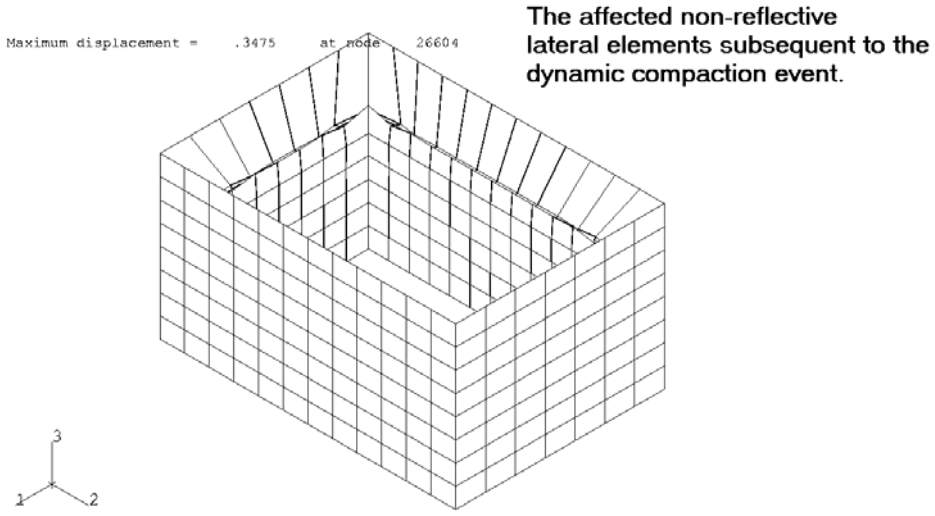

Figure 25. Affected non-reflective lateral elements subsequent to the dynamic compaction event

Colorized version of compacted soil layer. Red indicates maximum deformation. Blue indicates minimum deformation.

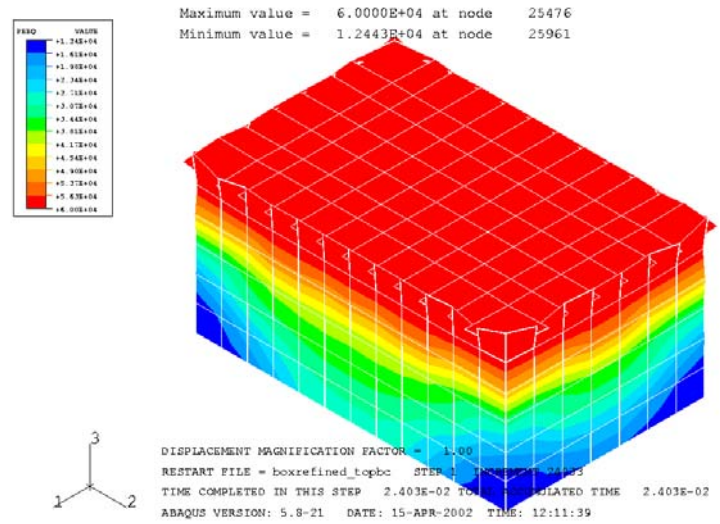

Figure 26. Colorized version of soil layer deformation

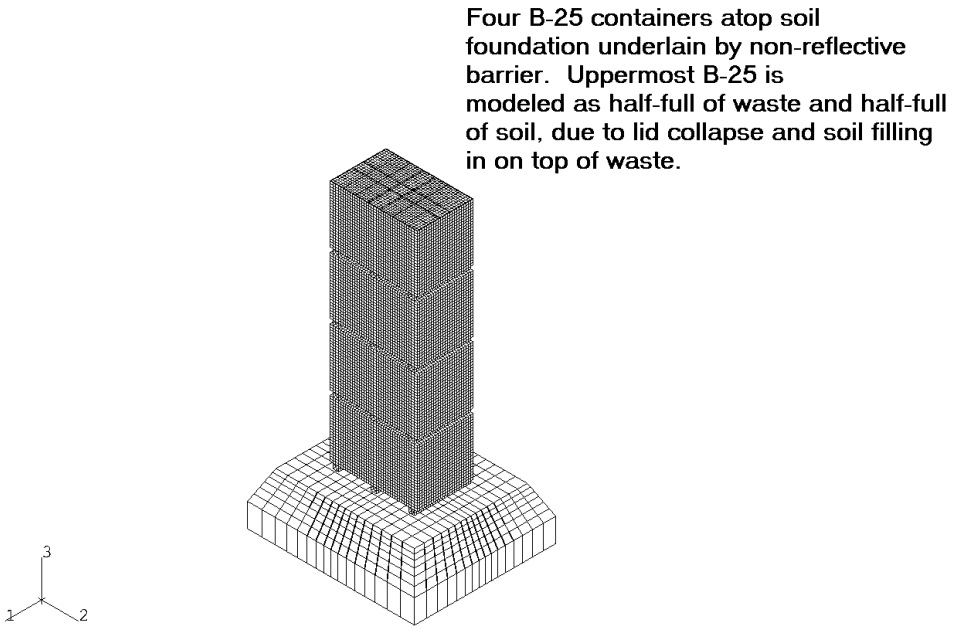

Figure 27. Four B-25s modeled with uppermost B-25 half-full of soil, half-full of waste, with soil foundation underlain by non-reflective barrier

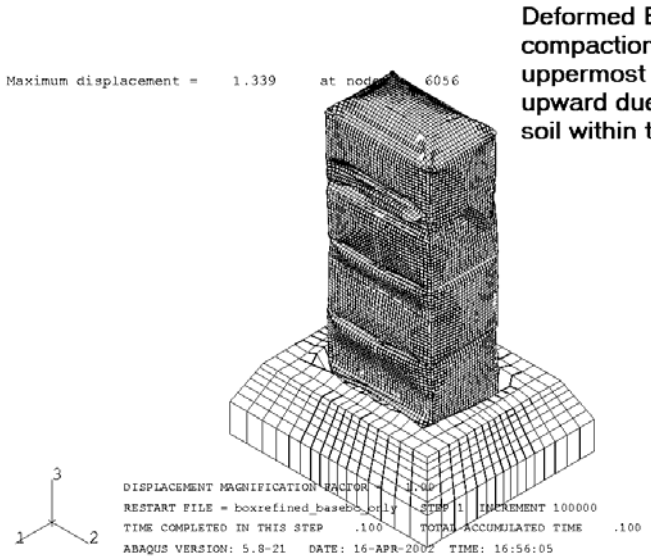

Figure 28. Deformed B-25s after dynamic compaction event. Uppermost B-25 appears to bulge upward due to presence of waste and soil within this B-25.

Top view of uppermost B-25. Top of B-25 appears to bulge upward due to presence of waste and soil within uppermost B-25.

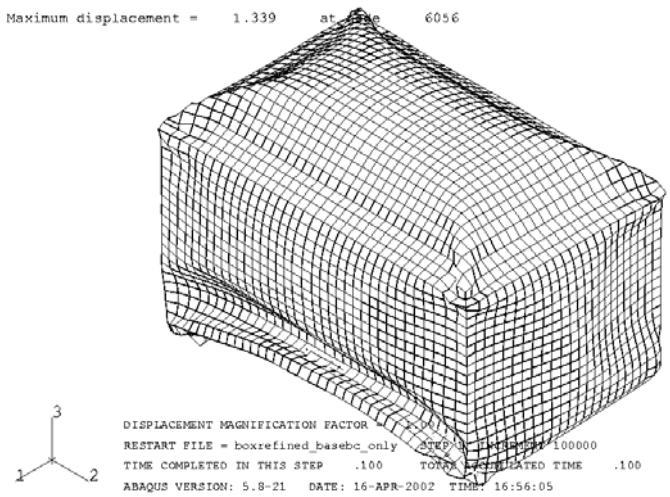

Figure 29. Top view of uppermost B-25. Top of B-25 appears to bulge upward due to presence of waste and soil within this B-25.

Bottom view of deformed uppermost B-25.

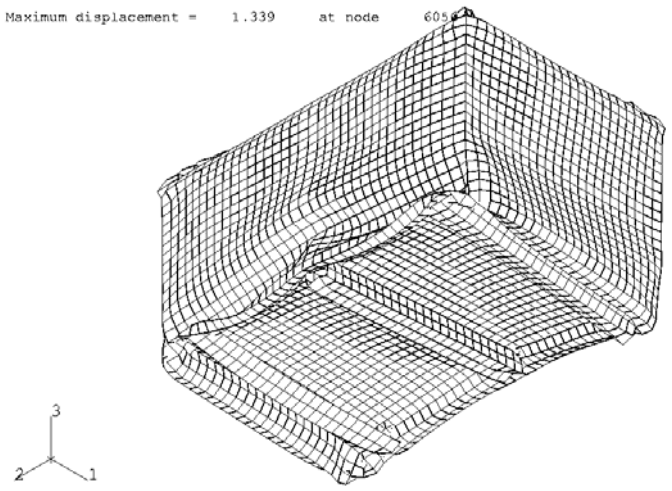

Figure 30. Bottom view of deformed uppermost B-25

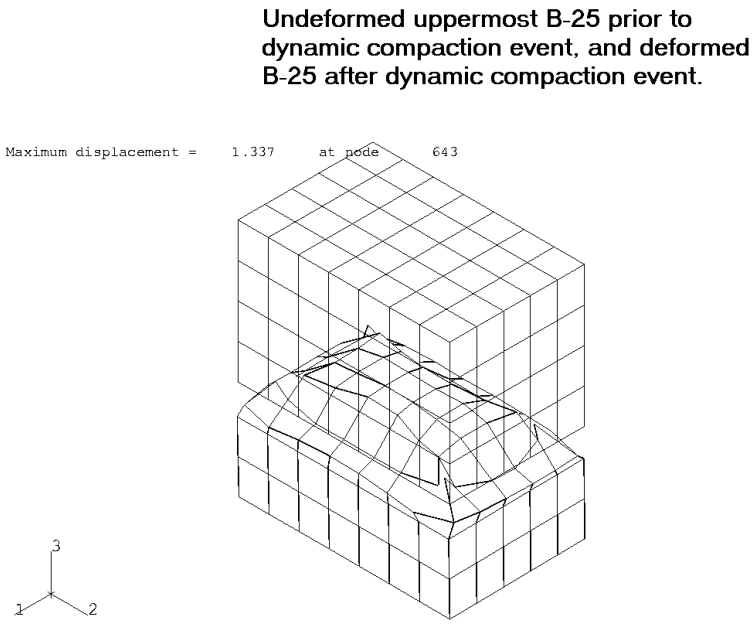

Figure 31. Undeformed uppermost B-25 prior to dynamic compaction event, and deformed uppermost B-25 after dynamic compaction event (includes waste in the bottom half and soil in the top half)

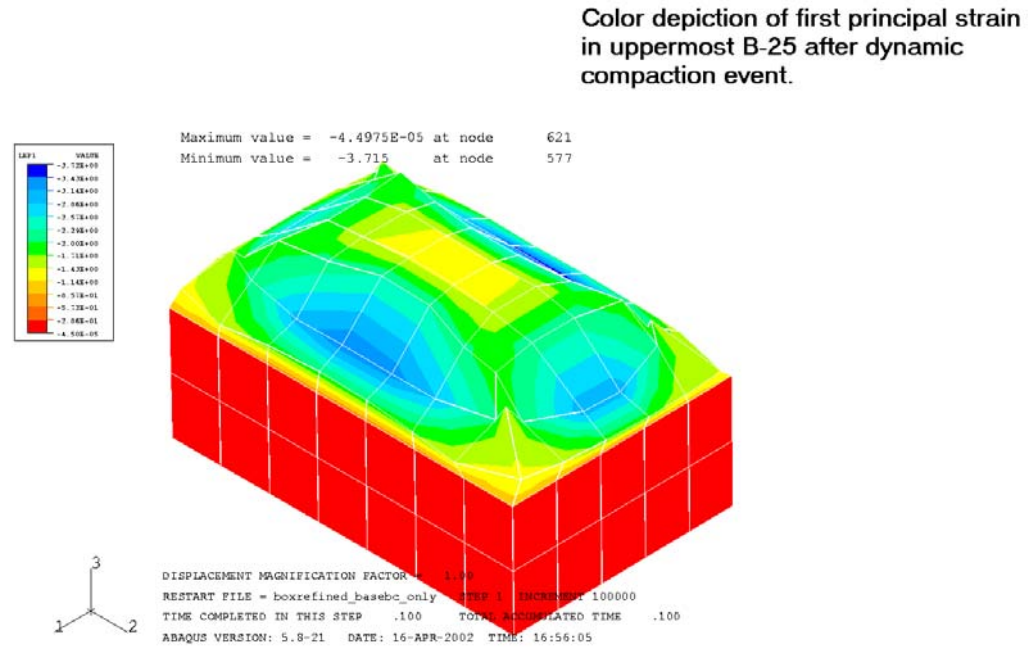

Figure 32. Color depiction of first principal strain in uppermost B-25 after dynamic compaction event (includes waste in the bottom half and soil in the top half)

2.3 INCORPORATING STEEL-VOLUME LOSS (CORROSION)

Addition of a “non-reflective” soil base to minimize the model-produced deformation of the lowermost B-25 enhanced the original efforts at structural finite element modeling related to dynamic compaction. An additional effort at enhancing the model incorporated steel-volume loss (i.e., corrosion), or “thinning” of some B-25 portions to evaluate changes in B-25 deformation with the same weight of compaction. Actual corrosion can result in a volume increase rather than a volume reduction. For modeling purposes, where loss of structural strength due to corrosion is modeled as a reduction in thickness of the B-25 steel, the term steel-volume loss is used. There are many different ways to achieve the same purpose. The thickness of the steel plate may be increased or decreased as the actual situation dictate. The strength reduction in the steel plate with corrosion can be modeled precisely provided that the true material properties of the corroded steel plate are available.

Figure 33through Figure 37 illustrate an example of the corrosion-related steel-volume loss refinement. Figure 33shows the results of a dynamic compaction event after the steel strength properties for the lowermost B-25’s top, bottom, risers, and sides have been reduced by 50 percent, and the second-from-lowermost B-25’s top, bottom, and risers strength properties have been reduced by 50 percent. The results are relatively greater compaction for the lower two B-25s compared to the results for B-25s with original steel thickness (compare to Figure 6, Figure 9, and Figure 28).

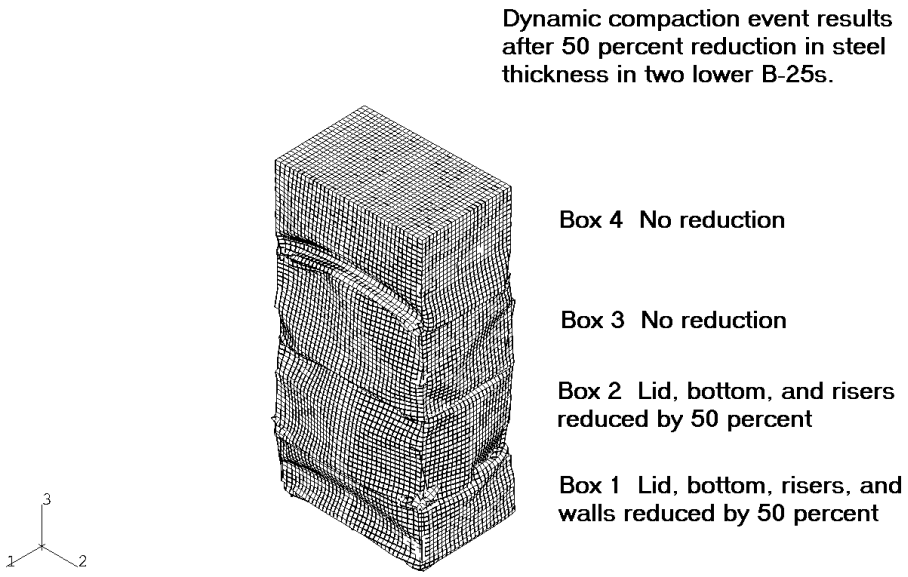

Figure 33. Dynamic compaction results after steel-volume reduction in lower two B-25s

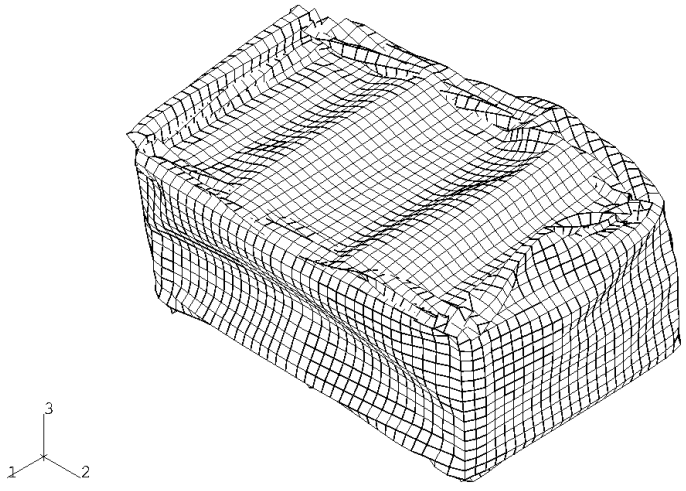

Figure 34. Top view of the lowermost B-25 (Box 1)

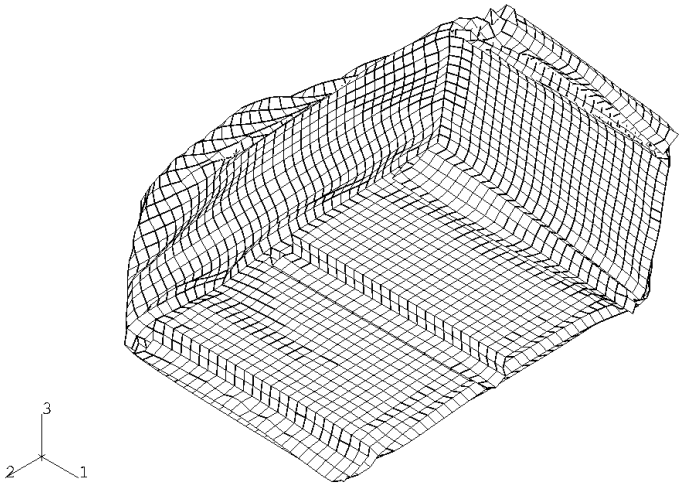

Figure 35. Bottom view of the lowermost B-25 (Box 1)

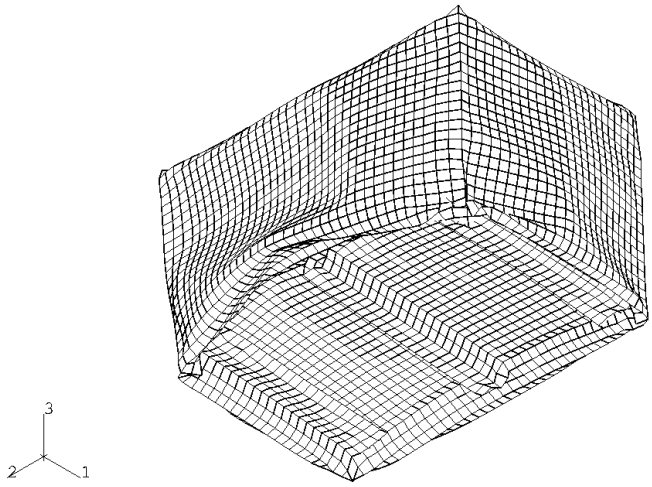

Figure 36. Bottom view of the second-from-bottom B-25 (Box 2)

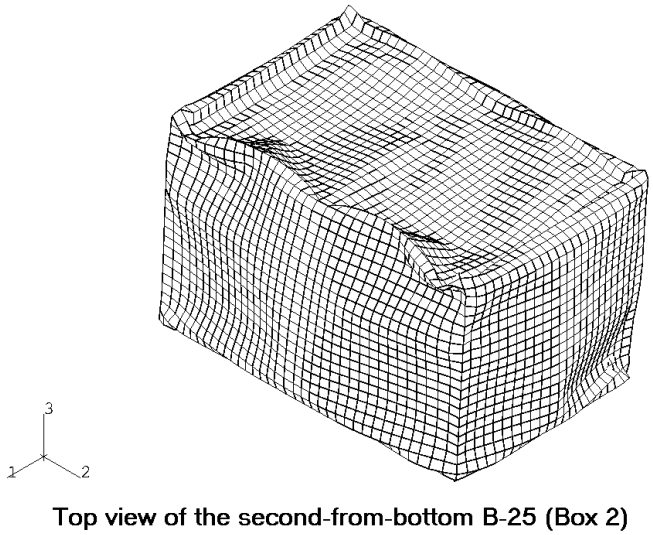

Figure 37. Top view of the second-from-bottom B-25 (Box 2)

3.0 CONCLUSIONS

Structural finite element modeling has successfully been used to depict the results of various B-25 disposal scenarios. Within the limitations of the modeling tools and the present computer capability extensive parametric studies have been performed. With the knowledge and experience gained through these studies, better solutions can be derived. Understanding the mechanical behaviors of the B-25 boxes will definitely enhance the future modeling of the overall subsidence of the Engineering Trench.

The initial feasibility and background evaluation for the dynamic compaction analysis are documented in Gong (2001), in which both geometric and material modeling are discussed. Also, static and quasi-static (dynamic analyses were suggested for developing constitutive equations for the B-25 boxes modeled as an amorphous material) analyses are suggested. Additional dynamic compaction related modeling is presented herein.

As the result of meetings with SRS Solid Waste Division, quasi-static modeling was initiated in spring of 2002. The quasi-static modeling results depict the results of B-25 steel-volume loss under static load conditions, and are presented in Wu (2002). With the quasi-static results, the complex details of the B-25 boxes can be modeled as amorphous material, such that the number of finite elements will be significantly reduced and consequently a finite element model for Engineering Trench #1 can be enlarged.

This report provides extensive modeling aspects of B-25 containers and enhances better understanding of the mechanical behavior of buried B-25s.

This page intentionally left blank.

4.0 REFERENCES

Dames and Moore, Inc., 1987. "Subsidence Study B-25 Metal Containers Mixed Waste Management Facility," DMSRP-97, March 4, 1997, letter report Charles T. Allen to Alex Guanlao, E. I. DuPont de Nemours & Company, Inc., Savannah River Plant, Aiken, SC 29808.

Gong, C., 2001, Finite Element Analysis of Dynamic Compaction of a Stack of Four B-25 Boxes (U), WSRC-TR-2001-00320, Westinghouse Savannah River Company, Aiken, SC 29808.

Jones, W.E., Li. W., 2001, Long-Term Waste Stabilization Parameter Estimation, Savannah River Site, Aiken, South Carolina (U), WSRC-TR-2001-00323, Westinghouse Savannah River Company, Aiken, SC 29808.

Wu, Tsu-Te, 2002 (draft). "Structural Analysis for Subsidence of Stacked B-25 Boxes (U)," WSRC-TR-2002-00378, Westinghouse Savannah River Company, Aiken, SC 29808.

Yau, W. W. F., 1986, "Structural Responses of B-25 Containers to Burial Ground Operation," DPST-86-335, letter report to J. R. Knight, March 14, 1986, Savannah River Laboratory, Aiken, SC 29808.

This page intentionally left blank.